WATER RESOURCES RESEARCH, VOL. 32, NO. 9, PAGES 2697–2703, SEPTEMBER 1996

Lognormal distribution model for unsaturated soil hydraulic properties

Ken'ichirou Kosugi

Laboratory of Erosion Control, Department of Forestry, Faculty of Agriculture, Kyoto University
Kyoto, Japan

Abstract. The soil water retention model developed by Kosugi was modified to be compatible with Mualem's model in order to derive an analytical expression for the relative hydraulic conductivity K_r. The modified water retention model is to be derived by applying a lognormal distribution law to the soil pore radius distribution function. Parameters of this retention model have physical significance on the water content (θ)–capillary pressure (ψ) curve and are related directly to the statistics of the pore radius distribution. The accuracy of the resulting combined water-retention-hydraulic-conductivity model is verified for observed data sets for six soils. Results showed that the proposed model produces acceptable matches with observed water retention curves and adequate predictions of hydraulic conductivities in five out of six cases. The $\theta - \psi$ and $K_r - \psi$ (or $K_r - \theta$) curves generated by this model are generally similar to those generated by van Genuchten's model.

Introduction

The hydraulic properties of unsaturated soil are represented by the relationship between the volumetric water content θ and the soil capillary pressure ψ and the relationship between the unsaturated hydraulic conductivity K and ψ. The $\theta - \psi$ relationship is referred to as the soil water retention curve. It is based on the soil pore radius (size) distribution.

Some models for water retention [e.g., *Brooks and Corey*, 1964; *van Genuchten*, 1980; *Russo*, 1988] have been developed to be compatible with models by *Burdine* [1953] and *Mualem* [1976a] for the purpose of deriving analytical expressions that can be used to predict the relative hydraulic conductivity of soil. The sets of the water retention model and the derived model for relative hydraulic conductivity are referred to as the combined water-retention-hydraulic-conductivity models and have been widely used for modeling purposes [e.g., *Russo et al.*, 1994; *Letha and Elango*, 1994]. These models are also useful for the inverse method to determine the soil hydraulic properties from transient data associated with unsaturated soil water flow [e.g., *Russo et al.*, 1991; *Toorman et al.*, 1992].

The combined water-retention-hydraulic-conductivity models have been frequently used for analyses of hysteretic phenomena found in the $\theta - \psi$ and $K - \psi$ relationships and spatial variability of soil hydraulic properties [e.g., *Luckner et al.*, 1989; *Russo and Bouton*, 1992]. Parameters of these models have been related to the soil texture and other soil properties such as bulk density and percentage of organic matter [e.g., *Clapp and Hornberger*, 1978; *Wösten and van Genuchten*, 1988]. *Mishra and Parker* [1990] and *Wise et al.* [1994] have analyzed the relationships between the saturated hydraulic conductivity and parameters of these models. Despite their usefulness these combined models use empirical curve-fitting equations for the soil water retention curve. They do not emphasize the physical significance of their empirical parameters.

On the other hand, *Brutsaert* [1966] applied several distribution laws to the model for the pore radius distribution and derived expressions for the soil water retention. By combining some of these water retention models with the *Childs and Collis-George* [1950] model, *Brutsaert* [1968] obtained some expressions for soil hydraulic conductivity. However, rather complicated forms of the derived conductivity models limited their usefulness for modeling purposes. Although *Laliberte* [1969] suggested his own distribution form for the soil pore radius distribution and derived a water retention model, the corresponding model for relative hydraulic conductivity was not developed. This study proposes a combined water-retention-hydraulic-conductivity model, which was developed by applying a distribution law available in general probability theory and which has a relatively simple functional form and hence can be effectively used both for analyses of soil hydraulic properties and for numerical models for processes in soils.

Recently, *Kosugi* [1994a] developed a soil water retention model by applying a three-parameter lognormal distribution law to the soil pore radius distribution function. Parameters of this retention model have physical significance on the $\theta - \psi$ curve and are related closely to the statistics of the pore radius distribution. It has been reported that this model performs as well as any existing empirical model for determining retention curves of various soils [*Kosugi*, 1994a, b], while the model has a relatively complicated functional form in comparison with widely used retention models. Applying a restriction to one of the parameters, this retention model is modified in this study to be compatible with *Mualem*'s [1976a] model in order to derive an analytical expression for the relative hydraulic conductivity. The accuracy of the resulting combined water-retention-hydraulic-conductivity model is verified for observed data sets for some soils having widely varying hydraulic properties.

Theory

Three-Parameter Lognormal Distribution Model for Soil Water Retention

The pore radius distribution function, $g(r)$, is defined as

$$g(r) = d\theta/dr \tag{1}$$

Paper number 96WR01776.
0043-1397/96/96WR-01776$09.00

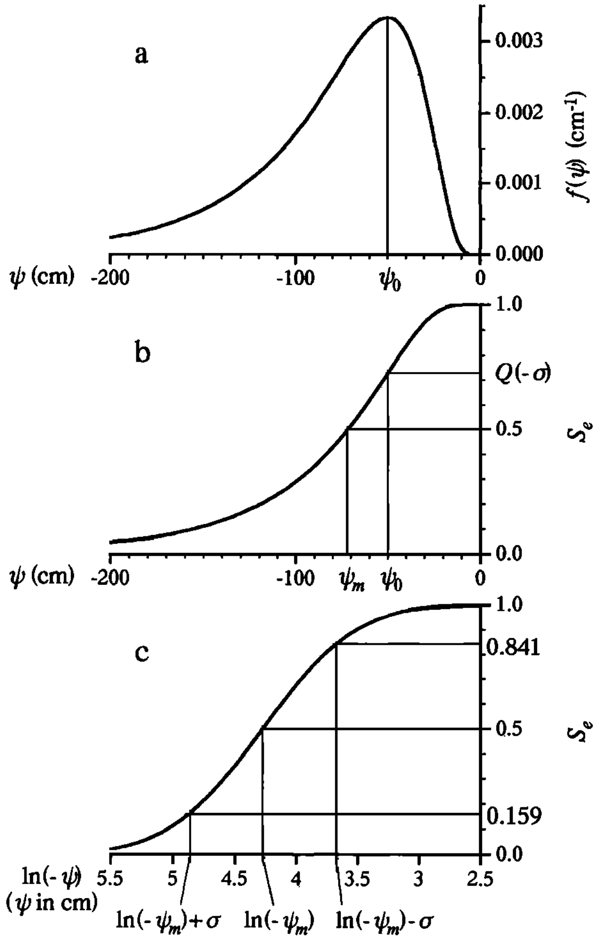

Figure 1. Curves for (a) $f(\psi) - \psi$, (b) $S_e - \psi$, and (c) $S_e - \ln(-\psi)$ based on the lognormal distribution model, showing plots of (9), (10), and (14) for $\psi_0 = -50$ cm, $\psi_m = -71.7$ cm ($\ln(-\psi_m) = 4.27$), $\sigma = 0.6$, $\theta_s = 0.4$, and $\theta_r = 0.1$.

where r is the pore radius. Consequently, $g(r)\, dr$ represents the volume of full pores of radii $[r, r + dr]$ per unit volume of medium. Here r is associated with ψ for a given saturation by the capillary pressure function

$$\psi = -2\gamma \cos \beta/\rho_w g r = A/r \tag{2}$$

where γ is the surface tension between the water and air, β is the contact angle, ρ_w is the density of water, and g is the acceleration of gravity. The constant value of $-2\gamma \cos \beta/\rho_w g = A = -0.149$ cm^2 [*Brutsaert*, 1966] is used in this study. On the basis of this direct correspondence of r and ψ, the distribution $g(r)$ is transformed into the distribution $f(\psi)$ by the following equation:

$$f(\psi) = g(r)\, dr/d\psi \tag{3}$$

Substituting (1) into (3) yields

$$f(\psi) = d\theta/d\psi \tag{4}$$

Hence $f(\psi)d\psi$ represents the volume of full pores in which water is retained by capillary pressure ψ to $\psi + d\psi$ per unit volume of medium. Therefore $f(\psi)$ can be regarded as the pore capillary pressure distribution function. From (4) it is evident that $f(\psi)$ is identical to the water capacity function.

Kosugi [1994a] obtained the following expression for $f(\psi)$ by applying a three-parameter lognormal distribution law to $g(r)$:

$$f(\psi) = \frac{\theta_s - \theta_r}{(2\pi)^{1/2}\,\sigma(\psi_c - \psi)} \cdot \exp\left\{-\frac{\left[\ln\left(\frac{\psi_c - \psi}{\psi_c - \psi_0}\right) - \sigma^2\right]^2}{2\sigma^2}\right\} \qquad \psi < \psi_c \tag{5}$$

$$f(\psi) = 0 \qquad \psi \geq \psi_c$$

where θ_s and θ_r are the saturated and residual water contents, respectively, and ψ_c, ψ_0, and σ are parameters. Parameter θ_r is defined as the water content when ψ is infinitely small, and the soil water conductivity is assumed to be zero. However, θ_r is commonly regarded as an empirical parameter. It is treated as one of the fitted parameters in this study. Parameter ψ_c is related to the maximum pore radius in the medium by (2) and ψ_0 is the mode of $f(\psi)$. Equation (5) has the three-parameter lognormal distribution form because the distribution of $\ln\{(\psi_c - \psi)/(\psi_c - \psi_0)\}$ obeys the normal distribution. Dimensionless parameter $\sigma(\sigma > 0)$ is the standard deviation of the distribution of $\ln\{(\psi_c - \psi)/(\psi_c - \psi_0)\}$. Because $\theta = \theta_r$ when $\psi = -\infty$, integrating (5) yields the following expression for water retention [*Kosugi*, 1994a]:

$$S_e = \frac{1}{2}\operatorname{erfc}\left\{\frac{\ln[(\psi_c - \psi)/(\psi_c - \psi_0)] - \sigma^2}{2^{1/2}\sigma}\right\} \qquad \psi < \psi_c \tag{6}$$

$$S_e = 1 \qquad \psi \geq \psi_c$$

where erfc denotes the complementary error function. S_e represents the effective saturation which is defined as

$$S_e = (\theta - \theta_r)/(\theta_s - \theta_r) \tag{7}$$

It has been reported that (6) exhibits great flexibility for determining retention curves of various soils [*Kosugi*, 1994a, b]. The other expression for (6) is

$$S_e = Q\{\ln[(\psi_c - \psi)/(\psi_c - \psi_0)]/\sigma - \sigma\} \qquad \psi < \psi_c \tag{6'}$$

$$S_e = 1 \qquad \psi \geq \psi_c$$

where Q is the complementary normal distribution function defined as

$$Q(x) = \int_x^\infty \frac{1}{(2\pi)^{1/2}} \exp\left(-\frac{x^2}{2}\right) dx \tag{8}$$

Two-Parameter Lognormal Distribution Model for Soil Water Retention

When the restriction of $\psi_c = 0$ is applied, (6) still produces acceptable matches with retention curves of soils which have no distinct bubbling pressure [*Kosugi*, 1994a]. With the restriction of $\psi_c = 0$, (5) and (6′) are transformed as follows:

$$f(\psi) = \frac{\theta_s - \theta_r}{(2\pi)^{1/2}\sigma(-\psi)} \exp\left\{-\frac{[\ln(\psi/\psi_0) - \sigma^2]^2}{2\sigma^2}\right\} \tag{9}$$

$$S_e = Q[\ln(\psi/\psi_0)/\sigma - \sigma] \tag{10}$$

Figures 1a and 1b show plots of (9) and (10), respectively, for $\psi_0 = -50$ cm, $\sigma = 0.6$, $\theta_s = 0.4$, and $\theta_r = 0.1$. The distribution expressed by (9) is not symmetrical. Notice that ψ_0 corresponds to the capillary pressure at the inflection point on the $S_e - \psi$ curve. The value of S_e at the inflection point is found by substituting $\psi = \psi_0$ into (10):

$$S_e(\psi_0) = Q(-\sigma) \tag{11}$$

Consequently, σ is the parameter which determines the value of $S_e(\psi_0)$. Small σ value reduces $S_e(\psi_0)$ value and makes the retention curve steep at the inflection point. This is confirmed by substituting $\psi = \psi_0$ into (9) to show that $f(\psi_0)$ becomes higher as σ decreases. The $S_e - \psi$ curve shown in Figure 1b has the $S_e(\psi_0)$ value of 0.73. The median of $f(\psi)$ expressed as (9) (ψ_m) is given by substituting $S_e = 0.5$ into (10):

$$\psi_m = \psi_0 \exp(\sigma^2) \tag{12}$$

Inverting (12) with respect to ψ_0 and substituting into (9) and (10) yields

$$f(\psi) = \frac{\theta_s - \theta_r}{(2\pi)^{1/2}\sigma(-\psi)} \exp\left\{-\frac{[\ln(\psi/\psi_m)]^2}{2\sigma^2}\right\} \tag{13}$$

$$S_e = Q[\ln(\psi/\psi_m)/\sigma] \tag{14}$$

Equation (13) has the lognormal distribution form since the distribution of $\ln(-\psi)$ obeys the normal distribution $N[\ln(-\psi_m), \sigma^2]$. Consequently, ψ_m is identical to the geometric mean of $f(\psi)$. A plot of (14) for $\psi_m = -71.7$ cm (that is, $\ln(-\psi_m) = 4.27$) and $\sigma = 0.6$ is shown using a semilogarithmic scale in Figure 1c. This ψ_m value is obtained from (12) by substituting $\psi_0 = -50$ cm and $\sigma = 0.6$ which are used for the $f(\psi) - \psi$ and $S_e - \psi$ curves shown in Figures 1a and 1b, respectively. It can be seen that ψ_m is identical to the capillary pressure at the inflection point on the $S_e - \ln(-\psi)$ curve. Notice that σ is equal to the difference between $\ln(-\psi_m)$ and the $\ln(-\psi)$ value at $S_e = 0.841$ or the difference between $\ln(-\psi_m)$ and the $\ln(-\psi)$ value at $S_e = 0.159$. Consequently, $S_e - \ln(-\psi)$ curve becomes steeper around the inflection point as σ becomes smaller. With a large σ value the curve has consistently small decreases in S_e as $\ln(-\psi)$ increases.

The pore radius distribution function $g(r)$ corresponding to the water retention model expressed as (14) is derived by substituting (2) and (13) into (3) and differentiating

$$g(r) = \frac{\theta_s - \theta_r}{(2\pi)^{1/2}\sigma r} \exp\left\{-\frac{[\ln(r/r_m)]^2}{2\sigma^2}\right\} \tag{15}$$

where r_m is the pore radius which is related to ψ_m by (2) (that is, $r_m = A/\psi_m$). Equation (15) represents a lognormal distribution since $\ln(r)$ obeys $N[\ln(r_m), \sigma^2]$. It should be noted that r_m is equal to the median and the geometric mean of $g(r)$. Parameter σ is related to the width of $g(r)$ since it is the standard deviation of the distribution of $\ln(r)$. Value of σ is small for a soil which has a narrow pore radius distribution and is large for a soil with a wide pore radius distribution.

Two-Parameter Lognormal Distribution Model for Relative Hydraulic Conductivity

Mualem's [1976a] model for predicting the relative hydraulic conductivity K_r from soil water retention curve is written in the form

$$K_r = K/K_s = S_e^{1/2}\left\{\int_0^{S_e}\frac{dS_e}{|\psi|}\bigg/\int_0^1\frac{dS_e}{|\psi|}\right\}^2 \tag{16}$$

where K_s and K are the saturated and unsaturated hydraulic conductivities, respectively. Combining (14) with (16) gives the functional relationships between K_r and S_e and K_r and ψ. The integral in (16) is transformed as follows:

$$\int_0^{S_e}\frac{dS_e}{|\psi|} = \frac{1}{\theta_s - \theta_r}\int_{\theta_r}^{\theta}\frac{d\theta}{|\psi|} = \frac{1}{\theta_s - \theta_r}\int_{-\infty}^{\psi}\frac{1}{|\psi|}f(\psi)\,d\psi$$

$$= \frac{1}{|A|(\theta_s - \theta_r)}\int_0^r rg(r)\,dr \tag{17}$$

When $g(r)$ is expressed as (15), the integration can be carried out without difficulties (see Appendix A):

$$\int_0^{S_e}\frac{dS_e}{|\psi|} = \frac{1}{|\psi_m|}\exp(\sigma^2/2)Q[\ln(\psi/\psi_m)/\sigma + \sigma] \tag{18}$$

Substituting $S_e = 1$ (that is, $\psi = 0$) into (18) yields

$$\int_0^1\frac{dS_e}{|\psi|} = \frac{1}{|\psi_m|}\exp(\sigma^2/2) \tag{19}$$

Hence (16) becomes

$$K_r = S_e^{1/2}\{Q[\ln(\psi/\psi_m)/\sigma + \sigma]\}^2 \tag{20}$$

By substituting (14) into (20), K_r can be expressed in the term of S_e or ψ:

$$K_r(S_e) = S_e^{1/2}\{Q[Q^{-1}(S_e) + \sigma]\}^2 \tag{21}$$

$$K_r(\psi) = \{Q[\ln(\psi/\psi_m)/\sigma]\}^{1/2}\{Q[\ln(\psi/\psi_m)/\sigma + \sigma]\}^2 \tag{22}$$

where Q^{-1} denotes the inverse function of Q defined as (8) and represents a percentage point of the normal distribution. The combination of the water retention model expressed as (10) or (14) and the hydraulic conductivity model expressed as (21) and (22) is referred to as the lognormal distribution model. Note that another expression for K_r can be derived by combining (14) with *Burdine*'s [1953] model for predicting the relative hydraulic conductivity (see Appendix B).

Plots of (21) for different σ values are shown using a logarithmic scale in Figure 2a. When $\sigma \to 0$, the medium has a uniform pore radius. It is clear from Figure 2a and also from (21) that for this case, K_r is expressed as a power function of S_e (that is, $K_r = S_e^{2.5}$) which is identical to the K_r model derived by applying the Kozeny equation [cf. *Kutílek and Nielsen*, 1994]. As σ becomes large, the ratio of change of K_r near saturation becomes great. Figure 2b shows the relationships between K_r and the reduced capillary pressure (ψ/ψ_m) obtained by (22) for different σ values. Actual ψ values are obtained by shifting the logarithmic scale by $\log(-\psi_m)$. With a small σ value, K_r remains near 1 for the small ψ/ψ_m value, and then there is an immediate sharp decline. With a large σ value the curve has consistently small decreases in K_r as ψ decreases.

Comparison With Experimental Data

To verify the accuracy of the lognormal distribution model, observed water retention curves and hydraulic conductivities for six soils were analyzed. Data sets for five soils have been already analyzed by *van Genuchten* [1980] using the combined water-retention-hydraulic-conductivity model suggested by himself. This model has been reported to perform relatively well in comparison with other models such as the Brooks and

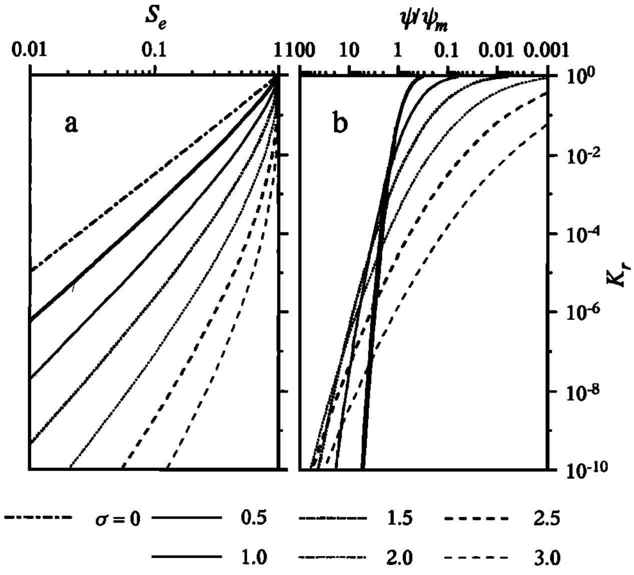

Figure 2. Curves for (a) $K_r - S_e$ and (b) $K_r - \psi/\psi_m$ based on the lognormal distribution model, showing plots of (21) and (22) for different σ values.

Corey model [*Brooks and Corey*, 1964] and has been used extensively in numerical modeling [*van Genuchten and Nielsen*, 1985; *Jury et al.*, 1991].

Van Genuchten's water retention model is

$$S_e = \{1 + (\alpha|\psi|)^n\}^{-m} \tag{23}$$

where α and n ($n > 1$) are parameters and m is related to n by $m = 1 - 1/n$ ($0 < m < 1$). Equation (23) can be transformed to include the capillary pressure at the inflection point on the $\theta - \psi$ curve (ψ_{0V}) which is given by differentiating (23) twice with respect to ψ (that is, $\psi_{0V} = -m^{1-m}/\alpha$) [*Kosugi*, 1994a]:

$$S_e = \{1 + m(\psi/\psi_{0V})^{1/1-m}\}^{-m} \tag{24}$$

Kosugi [1994a] has already shown (24) is analogous to (10) by analyzing the retention data sets for 50 soils. The residual sum of squares of the fitted versus observed water contents obtained by using both models for each retention data set resembled each other. For most data sets, ψ_{0V} took on nearly the same value as ψ_0 in (10). It has been also shown that the relationship between m and σ in (10) is expressed as

$$\sigma^2 = (1 - m) \ln \{(2^{1/m} - 1)/m\} \tag{25}$$

Equation (25) was obtained by assuming that the median of $f(\psi)$ based on the lognormal distribution model (ψ_m) (which is defined as (12)) is the same as that based on *van Genuchten*'s [1980] water retention model (ψ_{mV}); ψ_{mV} is given by substituting $S_e = 0.5$ into (24):

$$\psi_{mV} = \psi_{0V}\{(2^{1/m} - 1)/m\}^{1-m} \tag{26}$$

Van Genuchten [1980] substituted (23) into (16) and integrated to yield

$$K_r(S_e) = S_e^{1/2}\{1 - (1 - S_e^{1/m})^m\}^2 \tag{27}$$

$$K_r(\psi) = \frac{\{1 - (\alpha|\psi|)^{n-1}[1 + (\alpha|\psi|)^n]^{-m}\}^2}{\{1 + (\alpha|\psi|)^n\}^{m/2}} \tag{28}$$

$$(m = 1 - 1/n)$$

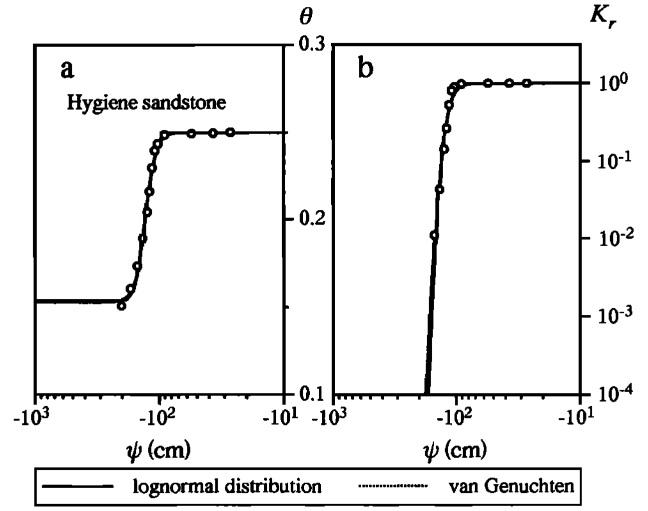

Figure 3. (a) Observed and fitted $\theta - \psi$ curves and (b) observed and predicted $K_r - \psi$ curves for Hygiene sandstone.

The combination of the water retention model expressed as (23) and the hydraulic conductivity model expressed as (27) and (28) is referred to as the van Genuchten model.

In Figures 3 through 7 the observed $\theta - \psi$ and $K_r - \psi$ curves for five soils taken from Mualem's catalog [*Mualem*, 1976b] are compared with the fitted $\theta - \psi$ and the predicted $K_r - \psi$ curves obtained by the lognormal distribution model. Parameters ψ_0, σ, and θ_r in (10) were optimized to fit the functional $\theta - \psi$ curves to the observed retention data sets using a nonlinear least squares optimization procedure based on Marquardt's maximum neighborhood method [*Marquardt*, 1963], and then ψ_m was computed by (12) using the estimated ψ_0 and σ. Applying Marquardt's method, the θ_s values were taken from Mualem's catalog. The $K_r - \psi$ curves were predicted by substituting the estimated ψ_m and σ into (22). The estimated parameters for each soil are summarized in Table 1 with the θ_s and K_s values taken from the catalog. The fitted $\theta - \psi$ and the predicted $K_r - \psi$ curves obtained by the *van*

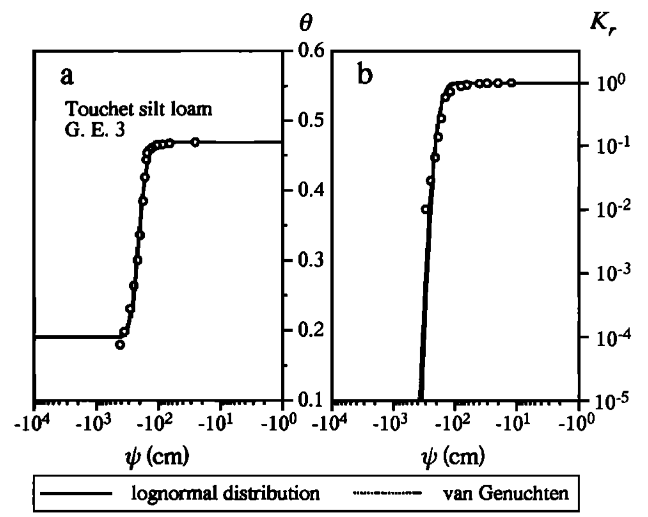

Figure 4. (a) Observed and fitted $\theta - \psi$ curves and (b) observed and predicted $K_r - \psi$ curves for Touchet silt loam G. E. 3.

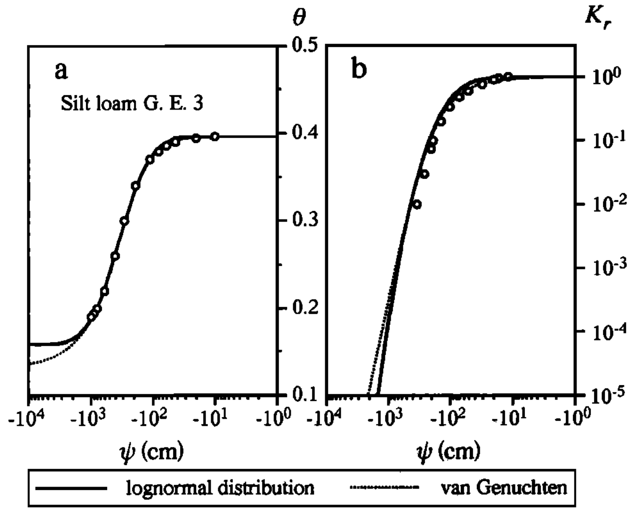

Figure 5. (a) Observed and fitted $\theta - \psi$ curves and (b) observed and predicted $K_r - \psi$ curves for Silt loam G. E. 3.

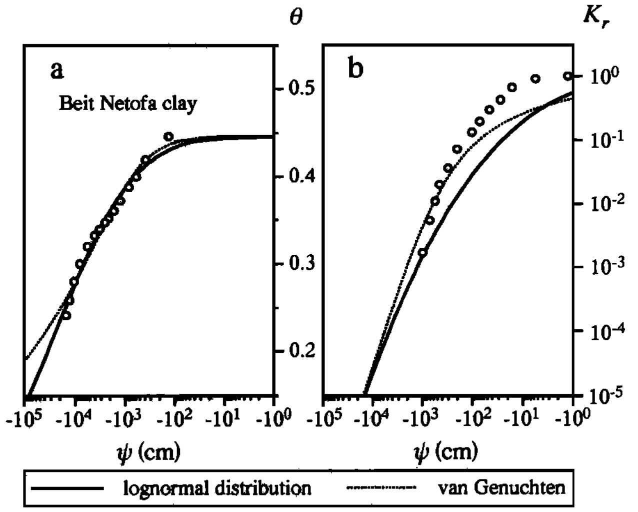

Figure 7. (a) Observed and fitted $\theta - \psi$ curves and (b) observed and predicted $K_r - \psi$ curves for Beit Netofa clay.

Genuchten [1980] model ((23) and (28)) are also shown in the figures. These curves were plotted using the estimated parameter values summarized in Table 1 of *van Genuchten* [1980], with the exception of the soil shown in Figure 6.

Figure 3 shows results obtained for Hygiene sandstone [*Brooks and Corey*, 1964] (Mualem's soil index 4130). The fitted $\theta - \psi$ curve generated by the lognormal distribution model matches the observed $\theta - \psi$ curve as well as the fitted curve by the *van Genuchten* [1980] model. Van Genuchten pointed out that a rather narrow pore radius distribution of this soil caused the water retention curve to become very steep at around $\psi = -125$ cm. This is clearly described by the estimated parameters of the lognormal distribution model: σ was estimated to be rather small ($\sigma = 0.16$), and the estimated ψ_0 value was -125 cm (Table 1). Figure 3b shows both the lognormal distribution and the van Genuchten models match the observed $K_r - \psi$ curve equally well.

Results for Touchet silt loam G. E. 3 [*Brooks and Corey*, 1964] (Mualem's soil index 3307) are given in Figure 4. Again, the lognormal distribution model performs quite well for the observed $\theta - \psi$ and $K_r - \psi$ curves.

Figure 5 shows results for Silt loam G. E. 3 [*Reisenauer*, 1963] (Mualem's soil index 3310). As *van Genuchten* [1980] pointed out, only a limited portion of the water retention curve was observed for this soil. This caused a difference between θ_r estimated by the lognormal distribution model and that estimated by the van Genuchten model. Two fitted curves resemble each other in the region where the observed retention data exist. The predicted $K_r - \psi$ curves by both models match the observed $K_r - \psi$ curve.

The data set for Gravelly sand G. E. 9 [*Reisenauer*, 1963] (Mualem's soil index 4135), shown in Figure 6, has not been analyzed by *van Genuchten* [1980]. Hence *Marquardt*'s [1963] method was used to fit (23) to the observed retention data set. Estimated values of θ_r, α, and n were 0.079, 0.0150 cm^{-1}, and 2.84, respectively. Again, the lognormal distribution model predicted the observed $K_r - \psi$ curve as well as the van Genuchten model.

In Figure 7, both the lognormal distribution and the *van Genuchten* [1980] models provide poor predictions of the $K_r - \psi$ curve observed for Beit Netofa clay [*Rawitz*, 1965] (Mualem's soil index 1006). Two predicted curves are slightly different from each other.

For illustration of a typical retention data set in which a hysteretic phenomenon is found, the observed data set for Guelph loam [*Elrick and Bowman*, 1964] is compared with the fitted $\theta - \psi$ and the predicted $K_r - \theta$ curves generated by the lognormal distribution model in Figure 8. The $\theta - \psi$ and $K_r - \theta$ curves generated by the van Genuchten model (Figure 9 of *van Genuchten* [1980]) are also shown in Figure 8. Marquardt's method was applied to optimize parameters in (10) for the observed retention data set using the same assumptions as van Genuchten did: θ_s for the wetting branch was assumed to be the highest measured value ($\theta_s = 0.434$), and θ_r for the wetting branch was assumed to be the same as θ_r estimated from the drying branch (see Table 1). In Figure 8b the $K_r - \theta$ curves predicted for the wetting branch were matched to the highest K_r value observed during the wetting process. It can be seen that the lognormal distribution model performs as well as

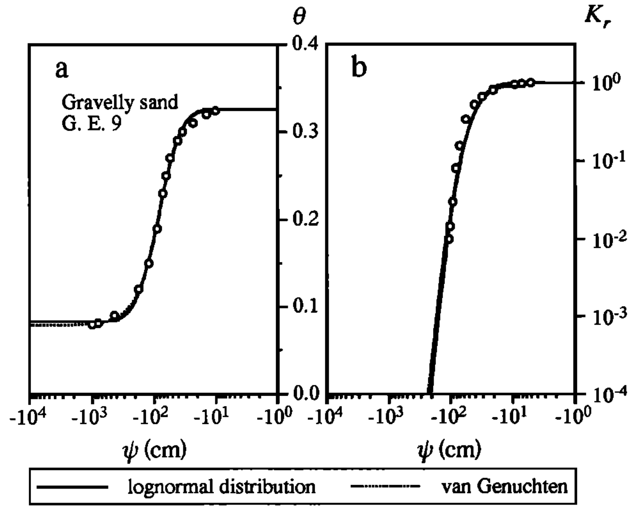

Figure 6. (a) Observed and fitted $\theta - \psi$ curves and (b) observed and predicted $K_r - \psi$ curves for Gravelly sand G. E. 9.

Table 1. Fitted Values for Parameters of the Lognormal Distribution Model for the Retention Curves Plotted in Figures 3 through 8

Soil Name	K_s,* cm/s	θ_s^*	θ_r	ψ_0, cm	ψ_m,† cm	σ
Hygiene sandstone	1.25E-3	0.250	0.154	−125.	−1.28E+2	0.161
Touchet silt loam G. E. 3	3.51E-3	0.469	0.191	−192.	−2.05E+2	0.253
Silt loam G. E. 3	5.74E-5	0.396	0.158	−150.	−3.47E+2	0.916
Gravelly sand G. E. 9	2.78E-4	0.326	0.083	−52.9	−8.35E+1	0.675
Beit Netofa clay	9.50E-7	0.446	0.000	−6.41	−2.42E+4	2.87
Guelph loam (drying)	3.66E-4	0.520	0.237	−52.3	−1.33E+2	0.966
Guelph loam (wetting)	···	0.434	0.237	−35.8	−5.46E+1	0.649

*Taken from Mualem's catalog [*Mualem*, 1976b].
†Computed by (12) using the estimated ψ_0 and σ.

the van Genuchten model for both drying and wetting branches of the $K_r - \theta$ curve.

Summary and Conclusions

In this study the soil water retention model proposed by *Kosugi* [1994a] was modified to be compatible with *Mualem*'s [1976a] model for the purpose of deriving an analytical expression for the relative hydraulic conductivity K_r. The accuracy of the resulting combined water-retention-hydraulic-conductivity model (the lognormal distribution model) was verified for observed data sets for six soils. Results showed that the lognormal distribution model produces acceptable matches with observed water retention curves and adequate predictions of hydraulic conductivities in five out of six cases. The $\theta - \psi$ and $K_r - \psi$ (or $K_r - \theta$) curves generated by this model are generally similar to those generated by *van Genuchten*'s [1980] model, which has been used extensively in numerical modeling.

The lognormal distribution model was developed by applying a lognormal distribution law to the soil pore radius distribution. The parameters of the model have physical significance on the $\theta - \psi$ curve: ψ_0 is the capillary pressure at the inflection point on the $\theta - \psi$ curve, and σ is a dimensionless parameter which decides the effective saturation S_e at the inflection point. The capillary pressure when S_e is equal to 0.5 (ψ_m) is expressed by the function with respect to ψ_0 and σ, and the model can be transformed to contain parameter ψ_m instead of ψ_0. Both ψ_m and σ have statistical significance on the soil pore radius distribution function $g(r)$: ψ_m is related to the median of $g(r)$ by the capillary pressure function and σ represents the width of $g(r)$. As a result the lognormal distribution model can be effectively used for analyses of soil hydraulic properties as well as for numerical models for processes in soils.

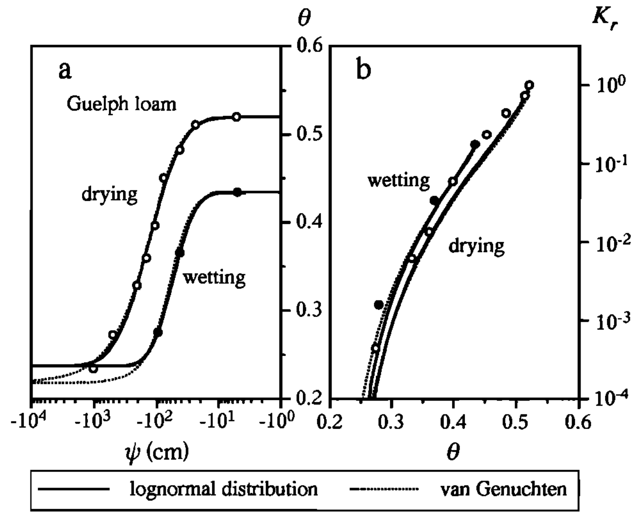

Figure 8. (a) Observed and fitted $\theta - \psi$ curves and (b) observed and predicted $K_r - \theta$ curves for Guelph loam.

Appendix A: Procedure for Deriving (18)

In order to derive analytical expressions for K_r based on *Mualem*'s [1976a] model, the following integral should be solved:

$$G = \frac{1}{\theta_s - \theta_r} \int_0^r r g(r)\, dr \tag{A1}$$

When $g(r)$ is expressed as (15), (A1) becomes

$$G = \frac{1}{(2\pi)^{1/2}\sigma} \int_0^r \exp\left\{-\frac{[\ln (r/r_m)]^2}{2\sigma^2}\right\} dr \tag{A2}$$

Substituting $y = \ln (r/r_m)$ into (A2) leads to

$$G = \frac{r_m}{(2\pi)^{1/2}\sigma} \int_{-\infty}^{\ln(r/r_m)} \exp (y - y^2/2\sigma^2)\, dy \tag{A3}$$

Substitution of $z = (\sigma^2 - y)/(2^{1/2}\sigma)$ into (A3) gives

$$G = \frac{r_m \exp (\sigma^2/2)}{-\pi^{1/2}} \int_{\infty}^{\{\sigma^2 - \ln(r/r_m)\}/2^{1/2}\sigma} \exp (-z^2)\, dz \tag{A4}$$

The error function (erf) is defined as

$$\operatorname{erf}(x) = \frac{2}{\pi^{1/2}} \int_0^x \exp (-x^2)\, dx \tag{A5}$$

Because erf $(\infty) = 1$, combining (A5) with (A4) yields

$$G = \frac{r_m \exp (\sigma^2/2)}{2} ((1 - \operatorname{erf} \{[\sigma^2 - \ln (r/r_m)]/2^{1/2}\sigma\})) \tag{A6}$$

Since the complementary normal distribution function (Q) is related to the error function by $\operatorname{erf}(x) = 1 - 2Q(2^{1/2}x)$, (A6) is transformed as

$$G = r_m \exp (\sigma^2/2) Q[\ln (r_m/r)/\sigma + \sigma] \tag{A7}$$

Substituting $r = A/\psi$ and $r_m = A/\psi_m$ into (A7) yields

$$G = \frac{A}{\psi_m} \exp(\sigma^2/2) Q[\ln(\psi/\psi_m)/\sigma + \sigma] \tag{A8}$$

Dividing (A8) by $|A|$ gives (18).

Appendix B: Equation for K_r Based on *Burdine*'s [1953] Model

Burdine's [1953] model for predicting K_r is written in the form

$$K_r = K/K_s = S_e^2 \int_0^{S_e} \frac{dS_e}{|\psi|^2} \bigg/ \int_0^1 \frac{dS_e}{|\psi|^2} \tag{A9}$$

The integral in (A9) is transformed as follows:

$$\int_0^{S_e} \frac{dS_e}{|\psi|^2} = \frac{1}{|A|^2(\theta_s - \theta_r)} \int_0^r r^2 g(r)\, dr \tag{A10}$$

When $g(r)$ is expressed as (15), (A10) can readily be integrated with the similar procedure as mentioned in Appendix A:

$$\int_0^{S_e} \frac{dS_e}{|\psi|^2} = \frac{1}{|\psi_m|^2} \exp(2\sigma^2) Q[\ln(\psi/\psi_m)/\sigma + 2\sigma] \tag{A11}$$

Consequently, K_r based on Burdine's model is expressed as

$$K_r = S_e^2 Q[\ln(\psi/\psi_m)/\sigma + 2\sigma] \tag{A12}$$

Acknowledgments. I express my gratitude to S. Kobashi, T. Mizuyama, and N. Ohte (all of Kyoto University) for valuable comments and criticisms of the manuscript. This research was partly supported by a grant from the Fund of Monbusyo for Scientific Research (07760151).

References

Brooks, R. H., and A. T. Corey, Hydraulic properties of porous media, *Hydrol. Pap. 3*, Civ. Eng. Dep., Colo. State Univ., Fort Collins, 1964.

Brutsaert, W., Probability laws for pore-size distributions, *Soil Sci.*, *101*, 85–92, 1966.

Brutsaert, W., The permeability of a porous medium determined from certain probability laws for pore size distribution, *Water Resour. Res.*, *4*(2), 425–434, 1968.

Burdine, N. T., Relative permeability calculation from size distribution data, *Trans. Am. Inst. Min. Metall. Pet. Eng.*, *198*, 71–78, 1953.

Childs, E. C., and N. Collis-George, The permeability of porous materials, *Proc. R. Soc. London A*, *201*, 392–405, 1950.

Clapp, R. B., and G. M. Hornberger, Empirical equations for some soil hydraulic properties, *Water Resour. Res.*, *14*(4), 601–604, 1978.

Elrick, D. E., and D. H. Bowman, Note on an improved apparatus for soil moisture flow measurements, *Soil Sci. Soc. Am. Proc.*, *28*, 450–453, 1964.

Jury, W. A., W. R. Gardner, and W. H. Gardner, *Soil Physics*, pp. 107–109, John Wiley, New York, 1991.

Kosugi, K., Three-parameter lognormal distribution model for soil water retention, *Water Resour Res.*, *30*(4), 891–901, 1994a.

Kosugi, K., Analysis of water retention curves of forest soils with three-parameter lognormal distribution model, *Nippon Rin Gakkaishi*, *76*(5), 433–444, 1994b.

Kutílek, M., and D. R. Nielsen, *Soil Hydrology*, pp. 104–105, Catena Verlag, Cremlingen, Germany, 1994.

Laliberte, G. E., A mathematical function for describing capillary pressure-desaturation data, *Bull. Int. Assoc. Sci. Hydrol.*, *14*(2), 131–149, 1969.

Letha, J., and K. Elango, Simulation of mildly unsaturated flow, *J. Hydrol.*, *154*, 1–17, 1994.

Luckner, L., M. T. van Genuchten, and D. R. Nielsen, A consistent set of parametric models for the two-phase flow of immiscible fluids in the subsurface, *Water Resour. Res.*, *25*(10), 2187–2193, 1989.

Marquardt, D. W., An algorithm for least-squares estimation of nonlinear parameters, *J. Soc. Ind. Appl. Math.*, *11*, 431–441, 1963.

Mishra, S., and J. C. Parker, On the relation between saturated conductivity and capillary retention characteristics, *Ground Water*, *28*(5), 775–777, 1990.

Mualem, Y., A new model for predicting the hydraulic conductivity of unsaturated porous media, *Water Resour. Res.*, *12*(3), 513–522, 1976a.

Mualem, Y., A catalogue of the hydraulic properties of unsaturated soils, *Proj. 442*, 100 pp., Technion-Israel Inst. of Technol., Haifa, Israel, 1976b.

Rawitz, E., The influence of a number of environmental factors on the availability of soil moisture to plants (in Hebrew), Ph.D. dissertation, Hebrew Univ., Rehovot, Israel, 1965.

Reisenauer, A. E., Methods for solving problems of multi-dimensional partially saturated steady flow in soils, *J. Geophys. Res.*, *68*, 5725–5733, 1963.

Russo, D., Determining soil hydraulic properties by parameter estimation: On the selection of a model for the hydraulic properties, *Water Resour. Res.*, *24*(3), 453–459, 1988.

Russo, D., and M. Bouton, Statistical analysis of spatial variability in unsaturated flow parameters, *Water Resour. Res.*, *28*(7), 1911–1925, 1992.

Russo, D., E. Bresler, U. Shani, and J. C. Parker, Analyses of infiltration events in relation to determining soil hydraulic properties by inverse problem methodology, *Water Resour. Res.*, *27*(6), 1361–1373, 1991.

Russo, D., J. Zaidel, and A. Laufer, Stochastic analysis of solute transport in partially saturated heterogeneous soil, 1, Numerical experiments, *Water Resour. Res.*, *30*(3), 769–779, 1994.

Toorman, A. F., P. J. Wierenga, and R. G. Hills, Parameter estimation of hydraulic properties from one-step outflow data, *Water Resour. Res.*, *28*(11), 3021–3028, 1992.

van Genuchten, M. T., A closed-form equation for predicting the hydraulic conductivity of unsaturated soils, *Soil Sci. Soc. Am. J.*, *44*, 892–898, 1980.

van Genuchten, M. T., and D. R. Nielsen, On describing and predicting the hydraulic properties of unsaturated soils, *Ann. Geophys.*, *3*(5), 615–628, 1985.

Wise, W. R., T. P. Clement, and F. J. Molz, Variably saturated modeling of transient drainage: Sensitivity to soil properties, *J. Hydrol.*, *161*, 91–108, 1994.

Wösten, J. H. M., and M. T. van Genuchten, Using texture and other soil properties to predict the unsaturated soil hydraulic functions, *Soil Sci. Soc. Am. J.*, *52*, 1762–1770, 1988.

K. Kosugi, Laboratory of Erosion Control, Department of Forestry, Faculty of Agriculture, Kyoto University, Kyoto 60601, Japan. (e-mail: f54174@sakura.kudpc.kyoto-u.ac.jp)

(Received October 9, 1995; revised March 28, 1996; accepted June 6, 1996.)